Initial Experiences with Artificial Neural Networks in the Detection of Computed Tomography Perfusion Deficits

Jan Vargas[1], *Alejandro Spiotta*[2], *Arindram Rano Chatterjee*[3]

BACKGROUND: **Head computed tomography (CT) with perfusion imaging has become crucial in the selection of patients for mechanical thrombectomy. In recent years, machine learning has rapidly evolved and found applications in a wide variety of health care tasks. We report our initial experiences with training a neural network to predict the presence and laterality of a perfusion deficit in patients with acute ischemic stroke.**

METHODS: **CT perfusion images of patients with suspicion for acute ischemic stroke were obtained. The data were split into training and validation sets. A long-term, recurrent convolutional network was constructed, which consisted of a convolutional neural network stacked on top of a long short-term memory layer.**

RESULTS: **Of the 396 patients, 139 (35.1%) had a right-sided perfusion deficit, 199 (50.3%) had a left-sided deficit, and 58 (14.6%) had no evidence of a deficit. The best model was able to achieve an accuracy of 85.8% on validation data. Receiver operating characteristic curves were generated for each class, and an area under the curve (AUC) was calculated for each class. For right-sided deficits, the AUC was 0.90, for left-sided deficits, the AUC was 0.96, and for no deficit, the AUC was 0.93.**

CONCLUSIONS: **The field of machine learning, powered by convolutional neural networks for the task of image recognition and processing, has quickly developed in recent years. We constructed an artificial neural network that can identify and classify the presence and laterality of a perfusion deficit on CT perfusion imaging.**

INTRODUCTION

Imaging has become an important tool within the field of medicine for the diagnosis and treatment of various diseases. Few specialties rely so heavily on computed tomography (CT) and magnetic resonance imaging (MRI) as the neurosciences. Within the field of stroke intervention, head CT scans with perfusion imaging have become crucial in the selection of patients for mechanical thrombectomy and have been proved to successfully aid in patient selection.[1-3] The desire for reliable and automated image recognition has led to the development of software packages such as the RAPID (iSchemaView, Redwood City, California, USA), which has been used to accurately identify the final stroke volume in patients with acute ischemic stroke. RAPID has been shown to accurately predict the final infarct volume from CT and MRI perfusion imaging studies using deconvolutional algorithms.[4]

In recent years, deep machine learning has rapidly evolved and found applications in a wide variety of health care tasks, such as automatic detection of colonic polyps, staging for lung cancer, and analyzing brain MRI studies for the presence of brain tumors.[5-12] Within the field of machine learning, convolutional neural networks (CNNs) have been shown to be well suited to image

Key words
- Acute ischemic stroke
- Artificial neural networks
- CT perfusion
- Machine learning

Abbreviations and Acronyms
3D: 3-Dimensional
AUC: Area under the curve
CNN: Convolutional neural network
DICOM: Digital Imaging and Communications in Medicine
LSTM: Long short-term memory
MRI: Magnetic resonance imaging
ROC: Receiver operating characteristic

From the [1]*Greenville Health System Division of Neuroendovascular Surgery, Greenville; and Departments of* [2]*Neurosurgery and* [3]*Radiology, Medical University of South Carolina, Charleston, South Carolina, USA*

To whom correspondence should be addressed: Jan Vargas, M.D. [E-mail: j.vargas.machaj@gmail.com]

Citation: World Neurosurg. (2019) 124:e10-e16. https://doi.org/10.1016/j.wneu.2018.10.084

*Journal homepage: **www.journals.elsevier.com/world-neurosurgery***

*Available online: **www.sciencedirect.com***

1878-8750/$ - see front matter Published by Elsevier Inc.

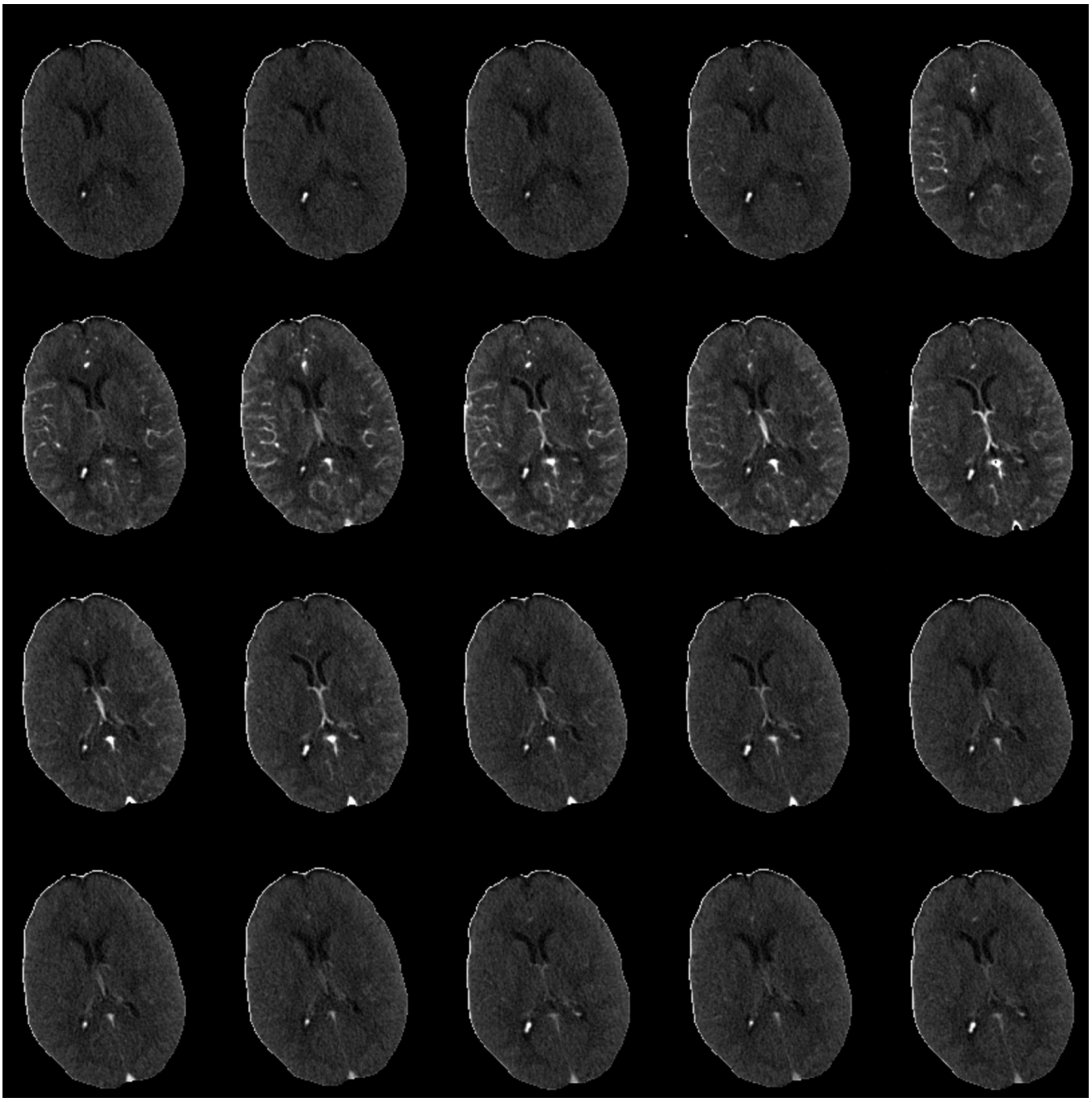

Figure 1. Representative collage of postprocessed images fed into the neural network showing 1 slice across 22 time steps in a patient with a left-sided occlusion. Delayed opacification of the left middle cerebral artery territory and delayed washout of contrast of the left middle cerebral artery territory were also present.

recognition and classification. These networks boast hundreds and, in some cases, thousands of convolutional layers and have demonstrated a top error rate of ~5% on certain image recognition tasks.[13,14] Such networks are well suited to image classification and workflow automation. We report our initial experience with training a neural network to predict the presence and laterality of a perfusion deficit in patients with acute ischemic stroke. This will lay the foundation for further work with

unsupervised machine learning using convolution and recurrent neural networks in the field of neuroimaging.

METHODS

Data Selection

A retrospective analysis of a prospectively maintained database was performed to identify all patients who had undergone thrombectomy for anterior circulation large vessel occlusion from December 2012 to April 2015 at our institution. We used an institutional review board–approved protocol. The CT perfusion scans and radiology reports of the selected patients were collected. At our institution, CT perfusion imaging is performed by obtaining contrast-enhanced CT head imaging with perfusion analysis using a 30-second delayed Omnipaque 350 iodinated contrast tracer and multiple acquisitions over time on Siemens CT scanners (Siemens Healthcare, Erlangen, Germany), with a slice thickness of 5 mm. These data are then postprocessed using the Siemens *syngo* Volume Perfusion CT Neuro package to obtain the mean transit time, time to peak, cerebral blood flow, and cerebral blood volume parametric maps. These are interpreted by attending neuroradiologists.

The radiology reports of the patients who had undergone mechanical thrombectomy were reviewed to determine the presence of a left- or a right-sided perfusion deficit. To qualify for mechanical thrombectomy, the patients were required to have a perfusion mismatch of $\geq$50% in the affected territory. Thus, this was used as a surrogate to select patients with a mismatch who had been deemed eligible candidates for thrombectomy. Each study was assigned a label according to the neuroradiologists' evaluation. Additionally, the radiology reports of the CT perfusion scans from May 2017 to September 2017 were reviewed. Any study for which the attending neuroradiologist had not reported a perfusion abnormality was collected and considered to show no deficit. Uninterpretable studies, because of poor bolus timing or motion artifact, were not included. The Digital Imaging and Communications in Medicine (DICOM) files of the contrast-enhanced CT head sequences with contrast tracer obtained over time (dynamic multiphase 4-dimensional [4D]) were collected for preprocessing.

Preprocessing Protocol

Each study's dynamic multiphase 4D DICOM files were used to construct 3-dimensional arrays of Hounsfield units extracted from the DICOM data and resampled into 1 mm × 1 mm × 1 mm isometric voxel volumes using spline interpolation along the z axis. We did not map the images to an atlas or use any motion correction. These were then segmented by choosing a Hounsfield range of 0–500 U, leaving only the brain parenchyma and contrast. We stacked the 3-dimensional (3D) arrays along the time axis, creating a 4D representation of each study in Hounsfield units. Variety was present in the size of the 3D studies and time steps owing to the different scanners used for acquisition; thus, to generate a uniform study size, we cropped the 4D array into studies with a resolution of 207 × 166 × 95 volumes distributed over 22 time steps (Figure 1). Data augmentation was used by randomly flipping studies along the z or y axis, or both. These arrays were normalized by feature scaling to a range of 0 to 1.

Table 1. Training Phase Data Sets

Data Set	Right	Left	Normal	Total
Training	124 (34.8)	182 (51.1)	50 (14)	356 (100)
Validation	15 (37.5)	17 (42.5)	8 (20)	40 (100)
Total	139 (35.1)	199 (50.2)	58 (14.6)	396 (100)

Data presented as n (%).
The training/validation split was 10%; no statistically significant difference was found in the frequency distribution between the 2 sets ($P = 0.478$).

Artificial Neural Network Architecture

A long-term, CNN was constructed consisting of a 3D-wide convolutional residual network (described by He et al.[13,14] and expanded on by Zagoruyko and Komodakis[15]) stacked on top of a long short-term memory (LSTM) layer. The 3D volume was used to extract the spatial features, and the outputs were sent to a global average pooling layer, followed by the LSTM layer over the time axis to extract the temporal features, and then classified into a left- or right-sided perfusion deficit or no deficit (**Supplemental Figure 1**).

The models were trained using a categorical cross-entropy loss, with an RMSprop optimizer. L2 weight regularization was used on convolutional layer kernels, and batch normalization was used throughout the model. Owing to the size of the individual data files and memory constraints, we opted to train on batch sizes of 6. Dropout layers were placed within the wide residual network block, as described by Zagoruyko and Komodakis[15,16] to aid with overfitting.

Network Training

For the training phase, the data set was initially randomly split into a training set consisting of 356 studies (90%) and a validation set of 40 studies (10%). The distribution of left, right, and no perfusion deficits was not significant between the initial training and validation sets ($P = 0.478$; **Table 1**). The network was tuned using the training set, with the validation set used as a holdout to monitor for overfitting. This training phase was performed for 150 epochs. Several combinations of network sizes were tested, with a network depth ranging from 2 to 4 and a widening factor of 4 or 6. Dropout values of 0.2, 0.3, and 0.4 were tested. Learning rate annealing was used, with a decrease in the learning rate after 30 epochs and no improvement in validation loss. The network was constructed using Keras, with Tensorflow backend, and run on an Arch Linux workstation with a Titan XP graphics processing unit donated by NVIDIA (Santa Clara, California, USA).

Network Validation

Once an optimal network had been trained, the entire data set was split into training and validation sets using stratified K-fold cross-

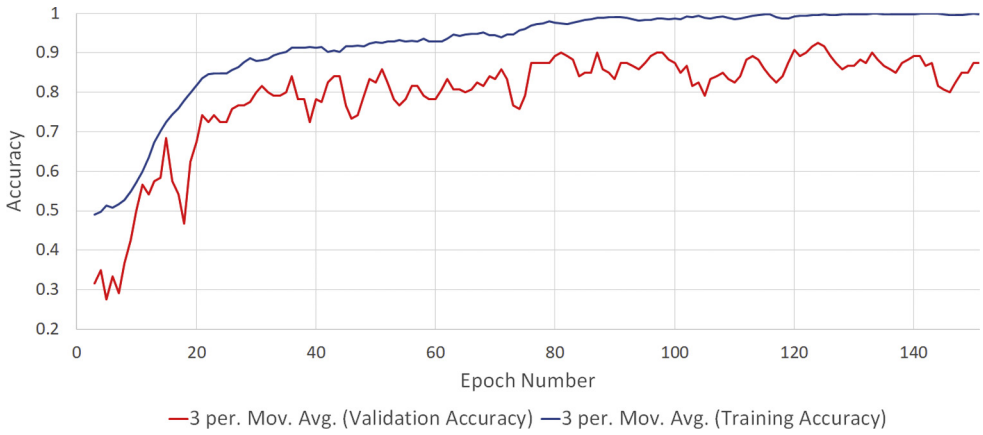

Figure 2. Training and validation accuracy over a number of epochs for the best model, represented as 3 period moving average (per. Mov. Avg.) trend lines during the training phase.

validation, with a K of 10. The best network was then validated over 10 folds, each consisting of 100 epochs, and the average accuracy was calculated.

Statistical Analysis

The scikit-learn python library was used to generate data sets for stratified K-fold cross validation. A χ^2 test for independence was performed on the distribution frequency of the initial training and validation sets, with P value of <0.05 considered statistically significant. Receiver operating characteristic (ROC) curves were generated for each of the 3 classes and an area under the curve (AUC) was calculated for each class using the best performing network.

RESULTS

A total of 396 perfusion series were reviewed and processed. Of the 396 patients, 139 (35.1%) had a right-sided perfusion deficit, 199 (50.3%) had a left-sided deficit, and 58 (14.6%) had no evidence of a deficit.

Six models were initially trained, with the best model achieving a validation accuracy of ~87.5% during the training phase. This model had an LSTM hidden layer size of 2048, a widening factor (k) of 6, a depth (n) of 4, and a dropout rate of 0.3 (Figure 2). The size of the LSTM hidden layer did not seem to affect the speed of the model convergence. The model depth appeared to reduce the validation loss, because models with a depth of 2 had a loss of almost twice as much as those with a depth of 4. Increasing the dropout rate also appeared to help with model convergence. Finally, increasing the widening factor also led to faster convergence. This model was validated using stratified K-fold cross validation for 10 folds on the entire data set, which yielded an average accuracy of 85.8% ± 0.118%.

ROC curves were created, and the AUC calculated. For right-sided deficits, the AUC was 0.90, for left-sided deficits, the AUC was 0.96, and for no deficit, the AUC was 0.93 (Figure 3).

DISCUSSION

Recent years have seen a significant growth in the field of machine learning, powered by advances in graphic processor unit technology and an abundance of training data. Within machine learning, artificial neural networks have received attention.[17-22] CNNs, which were described in 1998 by LeCun et al.,[23] are particularly well suited to process and extract features from images and have been expanded and successfully trained for image recognition tasks and segmentation.[24,25] The neurosciences have also been an attractive target for classification and segmentation tasks powered by CNNs. CNNs have been used in anatomy segmentation tasks on brain tumors or to detect and

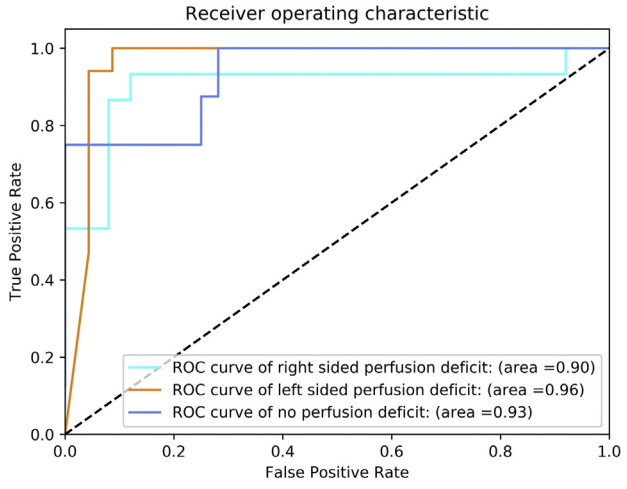

Figure 3. Receiver operating characteristic (ROC) curve for each diagnostic class examined (right-sided perfusion deficit, left-sided perfusion deficit, and no perfusion deficit), with an area under the curve for each class, generated using the best performing network.

segment a variety of brain lesions on MRI.[26-32] Additionally, work has been performed on accurate quantification of cerebrospinal fluid on non–contrast-enhanced head CT images.[33] Within the field of stroke, interest has been increasing in applying these methods to automate a variety of imaging-related tasks, such as the early detection of acute ischemic stroke or correctly identifying infarcted and hypoperfused tissue, predict the final infarct volume, or predict functional outcomes.[34-37]

Designing a Neural Network Architecture

In constructing our model, we decided to use deep artificial neural networks given the success of multilayered CNNs tasked with object recognition and classification. Much work has been done in the field of machine learning and computer vision; however, a comprehensive review was beyond the scope of the present study. For the present project, our task was to process studies consisting of 3D-CT volumes distributed along a time dimension. Sedaghat et al.[38] found that training a network to identify orientation in parallel improves performance. With CT scans, the difference in orientation will be minimal, because most patients will be placed in a similar orientation within the CT scanner; thus, this method would likely not improve performance. Another approach has been to train weak classifiers on both voxels and pixels and then construct an ensemble of the 2.[39] With respect to the time-distributed data, a variety of methods have been reported for the classification of videos, including using 2-stream CNNs on spatial and temporal features, which are represented as optical flows.[40-43] Using a 4D CNN for the analysis of a temporally distributed head CT scans was not computationally feasible with the present data set. LSTM networks, a variant of recurrent neural networks, have been used to process temporal data sequences and have found use in the field of natural language processing.[44-48] The addition of a temporal dimension to CT imaging with perfusion imaging made the use of an LSTM layer an attractive option, because the contrast bolus washing in and washing out over time provided the basis of the perfusion maps.

In several areas, our architecture could be improved. Most obviously, with the addition of more samples, we would expect the model would improve in performance. Additionally, transfer learning has been shown to improve performance in segmentation tasks in biomedical imaging and could be beneficial in this case, in addition to using pretrained architectures to extract 2-dimensional features, stacking those features, and feeding the 3D representation into an LSTM.[49-51] Assembling models and adding a support vector machine, in addition to the features extracted from a network, have been shown to also improve performance and are options for future improvements to our model.[24,52,53] Finally, by not cropping the time dimension and including the full study, more temporal information could be extracted. Despite not using conditional random fields for the 3D volume features or optical flows for temporal features and with minimal preprocessing, we were able to construct a relatively simple neural network with reasonable performance.

Clinical Implications

Our initial efforts yielded a neural network that achieved an accuracy of $\leq$85.8% after stratified K-fold cross-validation, with high AUC scores for each class, especially when tasked with identifying the presence or absence of a perfusion deficit (AUC, 0.93). The input to our network were the dynamic multiphase 4D sequences. Because the input into the model was the preprocessed Dyna CT data, there are potentially several features that the architecture could have used to classify the studies. Because the vessels were not segmented, 1 potential feature could be the detection of a large vessel occlusion, which would not require time-based analysis. Another feature could be Hounsfield unit attenuation over time in downstream microvascular territories. The network's predictions were tested against trained neuroradiologists' interpretations of the CT perfusion maps. This suggests that such models could aid in the timely detection of perfusion deficits. The present work represents our initial experience with artificial neural networks and serves as a proof-of-concept for an architecture and pipeline that could be used as the basis of future work.

Several software packages are available that assist in the detection of acute ischemic stroke and automatically calculate perfusion mismatch volumes and core infarct volumes via complicated mathematical algorithms such as the Brain CT Perfusion Package (Philips Healthcare, Eindhoven, The Netherlands), Syngo Volume Perfusion CT Neuro (Siemens Healthcare, Erlangen, Germany), and RAPID (iSchemaView, Redwood City, California, USA).[54] This software is based on work that was initially calculated using quantitative perfusion parameter maps from diffusion-weighted MRI.[55] RAPID CT perfusion defines the core infarct as a reduction in the relative cerebral blood flow to $<$30% of that in normal tissue and can redefine the thresholds of its outputs to generate new maps.[56] Such imposed parameters are a potential source of bias. RAPID's CT perfusion processing time ranges from 3 to 10 minutes; however, in 9% of cases, expert assessment overruled the RAPID mismatch classification.[57] Nonetheless, RAPID has been an essential and successful part of many recent clinical trials.[58-60] We believe that similar results can be achieved with CNNs, potentially by using the improvements discussed previously, and without the necessity of post-processing into perfusion maps. Although RAPID was not available at our institution, we believe that our pipeline could serve as the basis for future investigation comparing neural network-based classification of perfusion deficits.

Study Limitations

We acknowledge several limitations with the present study. The data set was weighted toward abnormal classes, with only 14.6% of the studies showing no perfusion deficits and more than one half (50.2%) of the studies representing a left-sided perfusion deficit. Nonetheless, our model was able to achieve a high AUC on the ROC curves and did not suffer from the accuracy paradox. The data set was manually selected, and we selected from a patient base deemed candidates for mechanical thrombectomy as a surrogate for detecting a perfusion mismatch with a $<$50% infarcted core. Although this introduced bias, the purpose of our model was to investigate architectures that could be used to classify patients into those with perfusion mismatches that could undergo intervention. As such, this approach serves to mirror our clinical practice. In contrast, our findings are limited by a single institution's approach to mechanical thrombectomy, and future studies are needed to validate the model using multicenter data. Finally, our model did not segment or calculate perfusion volumes

like other commercially available software packages. Future projects will serve to investigate these shortcomings.

CONCLUSION

The field of machine learning, powered by CNNs for the task of image recognition and processing, has quickly developed in recent years. By leveraging these new advances with the field of neuroimaging, we have constructed a simple artificial neural network that can identify and classify the presence of a perfusion deficit and the laterality on CT perfusion imaging studies. The present study serves as a proof-of-concept, highlighting 1 of the many possible uses for such technology, which we hope will ultimately assist in automating identification tasks and improving the time to diagnosis.

REFERENCES

1. Turk AS, Magarick JA, Frei D, Fargen KM, Chaudry I, Holmstedt CA, et al. CT perfusion-guided patient selection for endovascular recanalization in acute ischemic stroke: a multicenter study. *J Neurointerv Surg*. 2012;5:523-527.
2. Turk AS, Nyberg EM, Chaudry MI, Turner RD, Magarik JA, Nicholas JS, et al. Utilization of CT perfusion patient selection for mechanical thrombectomy irrespective of time: a comparison of functional outcomes and complications. *J Neurointerv Surg*. 2013;5:518-522.
3. Bouslama M, Haussen DC, Grossberg JA, Dehkharghani S, Bowen MT, Rebello LC, et al. Computed tomographic perfusion selection and clinical outcomes after endovascular therapy in large vessel occlusion stroke. *Stroke*. 2017;48:1271-1277.
4. Mokin M, Levy EI, Saver JL, Siddiqui AH, Goyal M, Bonafé A, et al. Predictive value of RAPID assessed perfusion thresholds on final infarct volume in SWIFT PRIME (solitaire with the intention for thrombectomy as primary endovascular treatment). *Stroke*. 2017;48:932-938.
5. Wolterink JM, Leiner T, de Vos BD, van Hamersvelt RW, Viergever MA, Isgum I. Automatic coronary artery calcium scoring in cardiac CT angiography using paired convolutional neural networks. *Med Image Anal*. 2016;34:123-136.
6. Jerebko AK, Summers RM, Malley JD, Franaszek M, Johnson CD. Computer-assisted detection of colonic polyps with CT colonography using neural networks and binary classification trees. *Med Phys*. 2003;30:52-60.
7. Georgiadis P, Cavouras D, Kalatzis I, Daskalakis A, Kagadis GC, Sifaki K, et al. Improving brain tumor characterization on MRI by probabilistic neural networks and non-linear transformation of textural features. *Comput Methods Programs Biomed*. 2008;89:24-32.
8. Kuruvilla J, Gunavathi K. Lung cancer classification using neural networks for CT images. *Comput Methods Programs Biomed*. 2014;113:202-209.
9. Toney LK, Vesselle HJ. Neural networks for nodal staging of non-small cell lung cancer with FDG PET and CT: importance of combining uptake values and sizes of nodes and primary tumor. *Radiology*. 2014;270:91-98.
10. Dusenberry MW, Brown CK, Brewer KL. Artificial neural networks: predicting head CT findings in elderly patients presenting with minor head injury after a fall. *Am J Emerg Med*. 2017;35:260-267.
11. Ibragimov B, Xing L. Segmentation of organs-at-risks in head and neck CT images using convolutional neural networks. *Med Phys*. 2017;44:547-557.
12. Nogueira MA, Abreu PH, Martins P, Machado P, Duarte H, Santos J. An artificial neural networks approach for assessment treatment response in oncological patients using PET/CT images. *BMC Med Imaging*. 2017;17:13.
13. He K, Zhang X, Ren S, Sun J. *Deep residual learning for image recognition*. ArXiv E-Prints; 2015:1512.
14. He K, Zhang X, Ren S, Sun J. *Identity mappings in deep residual networks*. ArXiv E-Prints; 2016:1603.
15. Zagoruyko S, Komodakis N. *Wide residual networks*. ArXiv E-Prints; 2016:1605.
16. Srivastava N, Hinton G, Krizhevsky A, Sutskever I, Salakhutdinov R. Dropout: a simple way to prevent neural networks from overfitting. *J Mach Learn Res*. 2014;15:1929-1958.
17. Badrinarayanan V, Kendall A, Cipolla R. SegNet: a deep convolutional encoder-decoder architecture for image segmentation. *IEEE Trans Pattern Anal Mach Intell*. 2017;39:2481-2495.
18. He K, Gkioxari G, Dollár P, Girshick R. Mask R-CNN. 2017 IEEE International Conference on Computer Vision. 2017:2980-2988.
19. Krizhevsky A, Sutskever I, Hinton GE. ImageNet classification with deep convolutional neural networks. *Commun ACM*. 2017;60:84-90.
20. Alvarez JM, Gevers T, LeCun Y, Lopez AM. Road scene segmentation from a single image. In: Fitzgibbon A, Lazebnik S, Perona P, Sato Y, Schmid C, eds. *Computer Vision—ECCV 2012*. Berlin: Springer; 2012:376-389.
21. Girshick R, Donahue J, Darrell T, Malik J. *Rich feature hierarchies for accurate object detection and semantic segmentation*. ArXiv E-Prints; 2014. arXiv: 1311.2524 [cs.CV].
22. Ren S, He K, Girshick RB, Sun J. Faster R-CNN: towards real-time object detection with region proposal networks. *CoRR*. 2015. arXiv:1506.01497 [cs.CV].
23. LeCun Y, Bottou L, Bengio Y, Haffner P. Gradient-based learning applied to document recognition. *Proc IEEE*. 1998;86:2278-2324.
24. Huang FJ, LeCun Y. Large-scale learning with SVM and convolutional for generic object categorization. Presented at the 2006 IEEE Computer Society Conference on Computer Vision and Pattern Recognition (CVPR'06), New York, NY, 2006:284-291. Available at: http://ieeexplore.ieee.org/stamp/stamp.jsp?tp=&arnumber=1640771&isnumber=34373. Accessed November 2017.
25. Ishii T, Nakamura R, Nakada H, Mochizuki Y, Ishikawa H. Surface object recognition with CNN and SVM in Landsat 8 images. Presented at the 2015 14th IAPR International Conference on Machine Vision Applications (MVA), Tokyo, 2015:341-344. Available at: http://ieeexplore.ieee.org/stamp/stamp.jsp?tp=&arnumber=7153200&isnumber=7153114. Accessed November 2017.
26. Kamnitsas K, Ledig C, Newcombe VFJ, Simpson JP, Kane AD, Menon DK, et al. Efficient multi-scale 3D CNN with fully connected CRF for accurate brain lesion segmentation. *Med Image Anal*. 2017;36:61-78.
27. Kamnitsas K, Chen L, Ledig C, Rueckert D, Glocker B. Multi-scale 3D convolutional neural networks for lesion segmentation in brain MRI. *Ischemic Stroke Lesion Segmentation*. 2015;13.
28. Payan A, Montana G. Predicting Alzheimer's disease: a neuroimaging study with 3D convolutional neural networks. *ArXiv Prepr*. 2015. ArXiv150202506.
29. Zhang W, Li R, Deng H, Wang L, Lin W, Ji S, et al. Deep convolutional neural networks for multi-modality isointense infant brain image segmentation. *Neuroimage*. 2015;108:214-224.
30. Kleesiek J, Urban G, Hubert A, Schwarz D, Maier-Hein K, Bendszus M, et al. Deep MRI brain extraction: a 3D convolutional neural network for skull stripping. *Neuroimage*. 2016;129:460-469.
31. Milletari F, Ahmadi S-A, Kroll C, Plate A, Rozanski V, Maiostre J, et al. Hough-CNN: deep learning for segmentation of deep brain regions in MRI and ultrasound. *Comput Vis Image Understanding*. 2017;164:92-102.
32. Akkus Z, Galimzianova A, Hoogi A, Rubin DL, Erickson BJ. Deep learning for brain MRI segmentation: state of the art and future directions. *J Digit Imaging*. 2017;30:449-459.
33. Patel A, van de Leemput SC, Prokop M, van Ginneken B, Manniesing R. Automatic cerebrospinal fluid segmentation in non-contrast CT images using a 3D convolutional network. *Int Soc Opt Photon*. 2017;10134:1013420.
34. Huang S, Shen Q, Duong TQ. Artificial neural network prediction of ischemic tissue fate in acute stroke imaging. *J Cereb Blood Flow Metab*. 2010;30:1661-1670.
35. Bagher-Ebadian H, Jafari-Khouzani K, Mitsias PD, Lu M, Soltanian-Zadeh H, Chopp M, et al. Predicting final extent of ischemic infarction using artificial neural network analysis of multi-

parametric MRI in patients with stroke. *PLoS One*. 2011;6:1-9.

36. Cuingnet R, Rosso C, Lehericy S, Dormont D, Benali H, Samson Y, et al. Spatially regularized SVM for the detection of brain areas associated with stroke outcome. *Med Image Comput Comput Assist Interv*. 2010;13(Pt 1):316-323.

37. Asadi H, Dowling R, Yan B, Mitchell P. Machine learning for outcome prediction of acute ischemic stroke post intra-arterial therapy. *PLoS One*. 2014;9:1-11.

38. Sedaghat N, Zolfaghari M, Amiri E, Brox T. Orientation-boosted voxel nets for 3D object recognition. 2016;ArXiv:1604.03351 [cs.CV]. Available at: http://arxiv.org/abs/1604.03351. Accessed January 26, 2018.

39. Hegde V, Zadeh R. FusionNet: 3D object classification using multiple data representations. *CoRR*. 2018. ArXiv:1707.06719v2 [cs.CV].

40. Chadha A, Abbas A, Andreopoulos Y. Video classification with CNNs: using the codec as a spatio-temporal activity sensor. *CoRR*. 2017. ArXiv:1710.05112v2 [cs.CV].

41. Ye H, Wu Z, Zhao R-W, Wang X, Jiang Y-G, Xue X. Evaluating two-stream CNN for video classification. *CoRR*. 2015. arXiv:1504.01920 [cs.CV].

42. Ji S, Yang M, Yu K. 3D convolutional neural networks for human action recognition. *IEEE Trans Pattern Anal Mach Intell*. 2013;35:221-231.

43. Karpathy A, Toderici G, Shetty S, Leung T, Sukthankar R, Fei-Fei L. Large-scale video classification with convolutional neural networks. In: Proceedings of the IEEE Conference on Computer Vision and Pattern Recognition. 2014:1725-1732.

44. Graves A, Schmidhuber J. Framewise phoneme classification with bidirectional LSTM and other neural network architectures. *Neural Netw*. 2005;18:602-610.

45. Mikolov T, Joulin A, Chopra S, Mathieu M, Ranzato M. Learning longer memory in recurrent neural networks. *ArXiv Prepr*. 2014. ArXiv:1412.7753 [cs.NE].

46. Sundermeyer M, Ney H, Schlüter R. From feedforward to recurrent LSTM neural networks for language modeling. *IEEEACM Trans Audio Speech Lang Process TASLP*. 2015;23:517-529.

47. Goldberg Y. A primer on neural network models for natural language processing. *J Artif Intell Res*. 2016;57:345-420.

48. Xiong W, Droppo J, Huang X, Seide F, Seltzer M, Stolcke A, et al. Achieving human parity in conversational speech recognition. *ArXiv Prepr*. 2016. ArXiv:160.05256.

49. Shin HC, Roth HR, Gao M, Lu L, Xu Z, Nogues I, et al. Deep convolutional neural networks for computer-aided detection: CNN architectures, dataset characteristics and transfer learning. *IEEE Trans Med Imaging*. 2016;35:1285-1298.

50. van Opbroek A, Ikram MA, Vernooij MW, de Bruijne M. Transfer learning improves supervised image segmentation across imaging protocols. *IEEE Trans Med Imaging*. 2015;34:1018-1030.

51. Huynh BQ, Li H, Giger ML. Digital mammographic tumor classification using transfer learning from deep convolutional neural networks. *J Med Imaging (Bellingham)*. 2016;3:034501.

52. Maji D, Santara A, Mitra P, Sheet D. Ensemble of deep convolutional neural networks for learning to detect retinal vessels in fundus images. *CoRR*. 2016. ArXiv:1603.04833.

53. Zhou Z-H, Jiang Y, Yang Y-B, Chen S-F. Lung cancer cell identification based on artificial neural network ensembles. *Artif Intell Med*. 2002;24:25-36.

54. Austein F, Riedel C, Kerby T, Meyne J, Binder A, Lindner T, et al. Comparison of perfusion CT software to predict the final infarct volume after thrombectomy. *Stroke*. 2016;47:2311-2317.

55. Straka M, Albers GW, Bammer R. Real-time diffusion-perfusion mismatch analysis in acute stroke. *J Magn Reson Imaging*. 2010;32:1024-1037.

56. Haussen DC, Dehkharghani S, Grigoryan M, Bowen M, Rebello LC, Nogueira RG. Automated CT perfusion for ischemic core volume prediction in tandem anterior circulation occlusions. *Interv Neurol*. 2016;5:81-88.

57. Campbell BCV, Yassi N, Ma H, Sharma G, Salinas S, Churilov L, et al. Imaging selection in ischemic stroke: feasibility of automated CT-perfusion analysis. *Int J Stroke*. 2014;10:51-54.

58. Campbell BC, Mitchell PJ, Kleinig TJ, Dewey HM, Churilov L, Yassi N, et al. Endovascular therapy for ischemic stroke with perfusion-imaging selection. *N Engl J Med*. 2015;372:1009-1018.

59. Saver JL, Goyal M, Bonafe A, Diener HC, Levy EI, Pereira VM, et al. Solitaire™ with the intention for thrombectomy as primary endovascular treatment for acute ischemic stroke (SWIFT PRIME) trial: protocol for a randomized, controlled, multicenter study comparing the Solitaire revascularization device with IV tPA with IV tPA alone in acute ischemic stroke. *Int J Stroke*. 2015;10:439-448.

60. Lansberg MG, Straka M, Kemp S, Mlynash M, Wechsler LR, Jovin TG, et al. MRI profile and response to endovascular reperfusion after stroke (DEFUSE 2): a prospective cohort study. *Lancet Neurol*. 2012;11:860-867.

Conflict of interest statement: The authors declare that the article content was composed in the absence of any commercial or financial relationships that could be construed as a potential conflict of interest.

Received 31 July 2018; accepted 15 October 2018

Citation: World Neurosurg. (2019) 124:e10-e16.
https://doi.org/10.1016/j.wneu.2018.10.084

Journal homepage: ***www.journals.elsevier.com/world-neurosurgery***

Available online: ***www.sciencedirect.com***

1878-8750/$ - see front matter Published by Elsevier Inc.